Graphical Abstract

Deuterium ion implantation of Eurofer with a new pulsed DC plasma source

J. A. Pittard[a,b*], J. A. Smith[b], A. Zafra[c], E. Martínez-Pañeda[c], N. A. Fox[b]

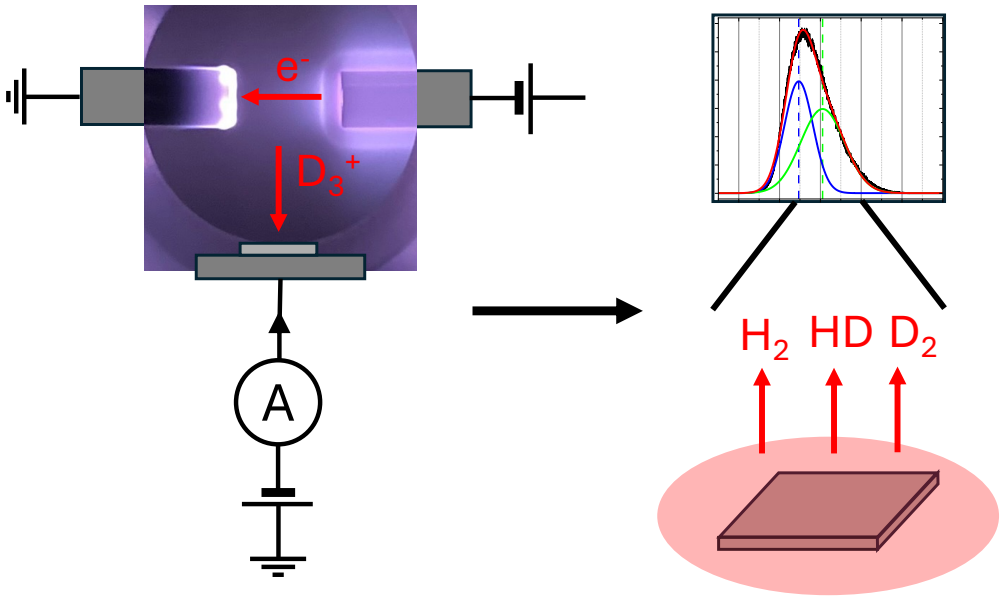

Highlights

Deuterium ion implantation of Eurofer with a new pulsed DC plasma source

J. A. Pittard[a,b*], J. A. Smith[b], A. Zafra[c], E. Martínez-Pañeda[c], N. A. Fox[b]

- A new setup (ExTEnD) for low energy deuterium ion exposure has been assembled
- ExTEnD can reach ion energies of 400 eV at a flux of 10^{18} m^{-2} s^{-1}
- Retention results of Eurofer were in good agreement with literature
- Total retained deuterium dominated by exposure time

Deuterium ion implantation of Eurofer with a new pulsed DC plasma source

J. A. Pittard[a,b*], J. A. Smith[b], A. Zafra[c], E. Martínez-Pañeda[c], N. A. Fox[b]

[a]*UKAEA, Culham Campus, Abingdon, UK,*
[b]*School of Physics, University of Bristol, Tyndall Avenue, Bristol, BS8 1TL, UK,*
[c]*School of Chemistry, University of Bristol, Cantock's Close, Bristol BS8 1TS, UK,*
[d]*Department of Engineering Science, University of Oxford, Oxford, OX1 3PJ, UK,*

Abstract

A new low energy ion source was developed. ExTEnD (Exposure to Low Energy Deuterium) uses an electrical discharge to create a plasma from which ions can be extracted via a biased sample stage - offering a simple and accessible setup to perform low energy ion exposure for hydrogen retention studies. Careful selection of operating conditions allowed stage current measurements to be used to estimate fluence, whilst the bias applied to the stage dictated the incident ion energy. The design and testing of ExTEnD is presented, alongside a preliminary study in which ion flux incident on Eurofer samples was varied in two ways. Thermal desorption results were broadly in good agreement with a variety of other studies, with three commonly observed desorption peaks present across the samples. The longer exposure time of the lowest flux sample resulted in a notable increase in retained deuterium.

Keywords: Hydrogen, Retention, Plasma Facing Material

1. Introduction

One of the key challenges facing the success of commercial fusion reactors is the selection of appropriate plasma facing materials (PFMs). Such a material must withstand high fluxes of fast neutrons, high thermal loads and an interaction with hydrogen ions. The deuterium and tritium ions used in fusion can react with the PFM in a number of different ways. Ions may permeate through the material (raising concerns over contamination and structural defects such as bubbles [1]), desorb from the material back into the plasma (known as recycling, results in cooling of the plasma) or

simply be retained within the material (resulting in embrittlement in some materials, increasing the start-up tritium inventory and the need for detritiation during decommissioning [2, 3]). Therefore, the retention mechanisms of any proposed PFM, as well as other materials within a fusion reactor, must be understood and experimental setups are required to do so. A variety of different techniques have been developed to explore the interaction between hydrogen isotopes and materials.

- Ion implantation - Although some lower energy ion beams have been used in retention studies [4, 5], typically, the energy range of an ion beam ($10^3 - 10^6$ eV) is orders of magnitude higher than the energy of ions incident on a PFM (10^1 eV) and therefore inappropriate. More specialised plasma-based setups have also been created [6, 7, 8], in which ions are extracted from a low temperature plasma at energies of $10^1 - 10^3$ eV.

- Electrochemical charging - A bias is applied to a conductive sample submerged in a solution containing hydrogen ions [9]. Ions will saturate the surface and, over time, diffuse into the material.

- Gas permeation - The sample is exposed to a hydrogen gas at elevated temperature and pressure. This method is commonly used to determine diffusion coefficients and permeation rates [10].

To explore retention of hydrogen isotopes in PFMs and other fusion relevant materials, a new low energy ion source has been assembled at the University of Bristol. Ions in ExTEnD (EXposure To low ENergy Deuterium) are extracted from a plasma formed via electrical discharge. In contrast to similar setups which use a microwave plasma, ExTEnD is a more accessible setup in terms of both simplicity and cost, whilst still maintaining good separation from the plasma, resulting in negligible sample heating and accurate measurement of ion energy and fluence which can be challenging in glow discharge setups. Reliance on an electrical discharge meant careful selection of operating conditions was required. This work outlines the basic design and determination of operating conditions. More information on the design, assembly and testing of the setup can be found in [11]. To verify ExTEnD, a preliminary study is also presented, in which Eurofer samples are exposed at different fluxes.

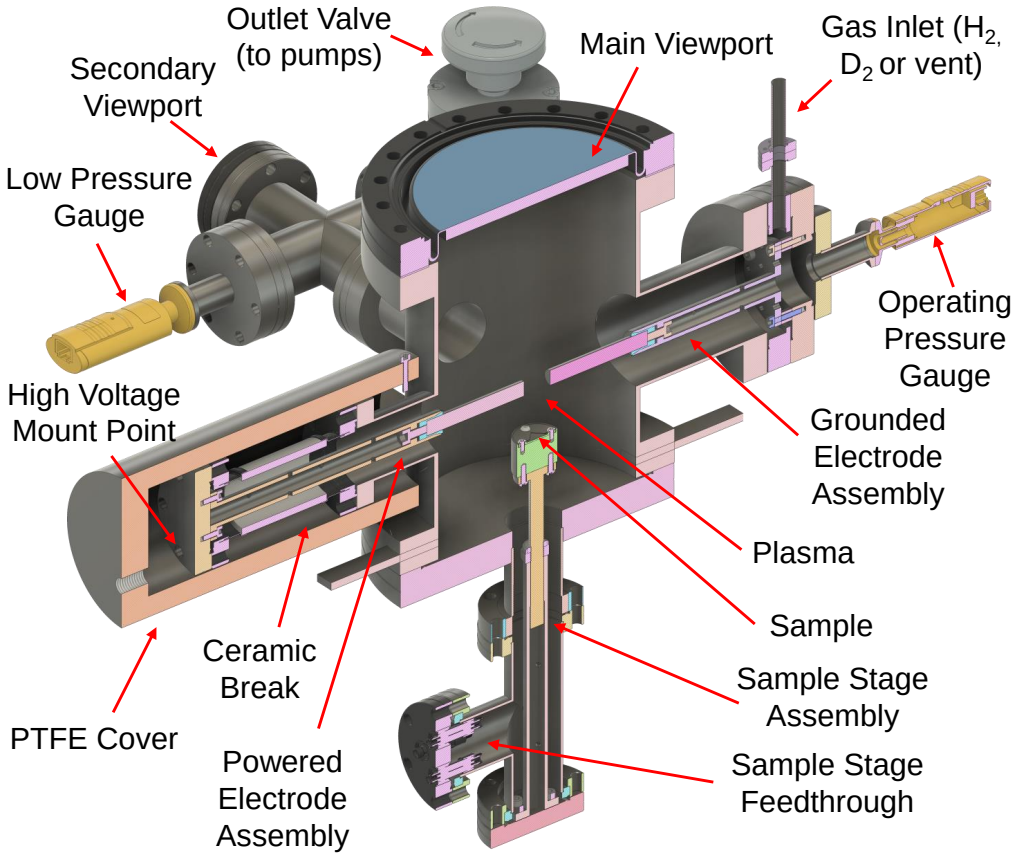

Figure 1: Diagram of ExTEnD with key parts indicated, as viewed from the back.

2. A new deuterium ion source - ExTEnD

2.1. Design

The final design of ExTEnD can be seen in Fig. 1. Similar setups broadly consist of three main sections: a deuterium plasma, a way to extract ions at a known energy, and a sample stage to expose the sample at a measured fluence. In ExTEnD, the plasma is created via an electrical discharge between two electrodes, beneath which the sample stage is positioned. Applying a negative bias to the sample stage extracts ions from the plasma at an energy approximately equal to the bias applied (assuming a plasma potential of a few volts). In a manner similar to a Langmuir probe, measuring the current required to maintain the negative bias can be used to indicate the flux of

positive ions on the surface, allowing the fluence to be calculated. The use of a discharge plasma and biased stage allows for a relatively simple and accessible way of producing and extracting ions.

The electrodes consisted of two tungsten rods. Electrode mounts were machined from a single piece of stainless-steel and consisted of a mounting plate at the base of a hollow tube. A collet was used to secure the electrodes to the mount offering a secure fit, whilst maintaining parallel electrode faces and avoiding the need to alter the brittle tungsten. The length of the electrode mounts and electrodes was selected to give a 20 mm electrode gap. Spacers can also be used to decrease this gap to 15 mm if desired. The powered electrode was connected to the power supply via the external face of the blanking flange it was mounted on. The live face was covered with a PTFE cover for safety.

There were several key considerations surrounding the design of the sample stage beyond offering a secure mounting for the sample. The separation between plasma and sample stage impacts the flux of incident ions, the likelihood of a secondary plasma discharge forming on the stage, and the temperature of the sample. As such, the sample stage assembly was designed to allow the height to be adjusted. The top of the stage was electrically isolated from the sample stage mount to allow for the stage bias to be applied.

The different components of the sample stage can be seen in Fig. 2. The baseplate was machined from a single piece of stainless-steel and consisted of a disc with a threaded rod protruding out of the bottom. This threads into the sample stage mount, which takes a similar form to the high voltage electrode mount - a long stainless-steel tube mounted to a blanking flange. The internal top section of this tube is tapped. To adjust the height, the sample stage can be screwed in or out and secured in place with the locking nut. This design was simple and effective, but meant it was not possible to adjust the height during operation or under vacuum, and the sample stage must be removed to do this. This compromise was deemed acceptable as height adjustment was not expected to be required once standard operating conditions had been established.

The insulating block was made from MACOR - a machinable ceramic material, which isolates the biased sample stage from the grounded base plate it was mounted to. The sample stage consists of a sample plate and window plate, which sit in a recessed region within the insulating block. The sample plate has a square 11×11 mm^2, 1 mm recess in the centre to accommodate 10×10 mm^2 samples. The window plate is used to secure

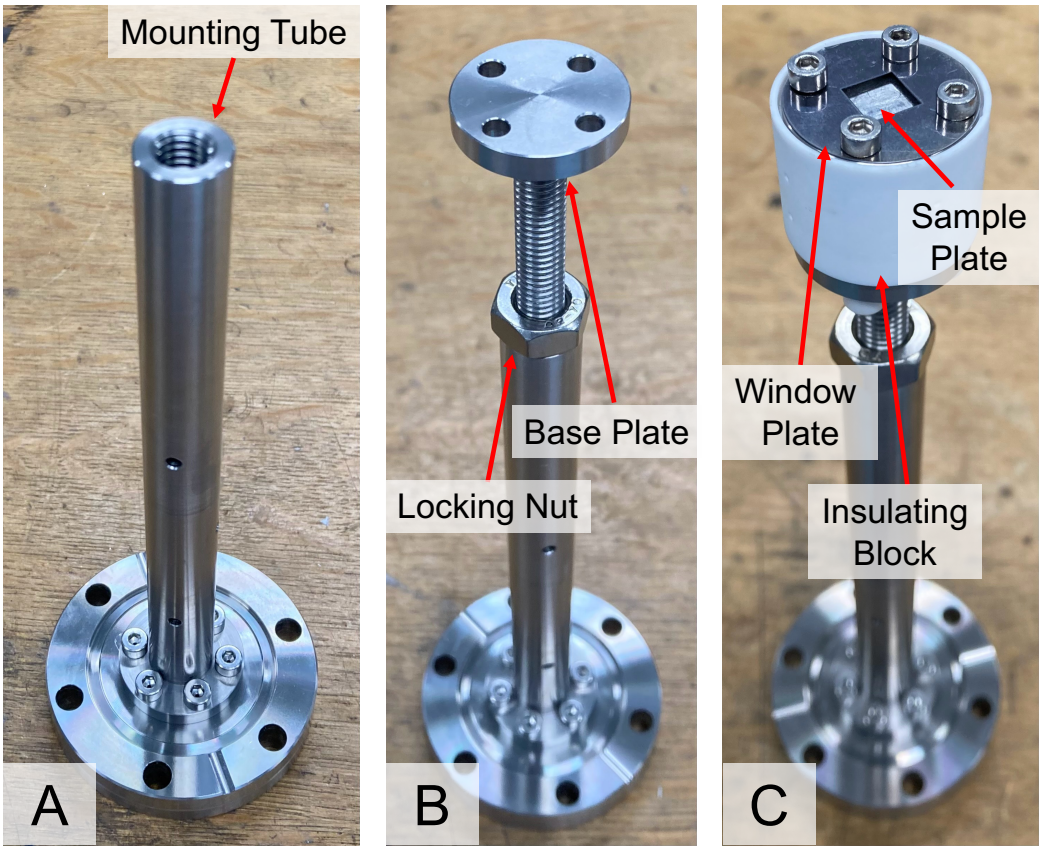

Figure 2: Sample stage assembly. **A** - Mounting tube affixed to blanking flange. **B** - Base plate and locking nut mounted. **C** - Mounted sample stage.

Table 1: The range of variables used in testing of the new implanter. Combinations of the above conditions were selected to explore trends.

Testing Parameters	
Pressure (Torr)	0.1, 0.2, 0.5, 1, 1.5, 2, 3, 5, 10, 20
Electrode Power (W)	40–80, 10 W increments
Stage Bias (-V)	0–800, 10–50 V increments
Stage-Electrode Separation (mm)	25, 35, 50, 65
Pulse t_{off} (µs)	0.1–0.45, 0.5 increments

the sample to the stage and give a defined implantation area. In the centre there is a square 8×8 mm^2 window, ensuring a 10×10 mm^2 sample will always have the same exposure area even if there is some lateral movement in the inset region. A laser cutter was used to cut out window plates from a tantalum foil and means different window sizes could easily be made for different samples. To load and unload samples, the tee at the bottom of the setup is removed and the sample stage assembly is withdrawn from the base. The window plate can then be removed, the sample placed in the recess of the sample plate, and the window plate reattached to secure the sample.

ExTEnD is run as a static volume, meaning no gas flow is present during operation. Compared to continuous flow systems, a static volume system is much simpler and reduces gas wastage significantly, meaning the 500 ml lecture bottle mounted to the frame is sufficient for 10s of exposures (when filled to a few bar of D_2). The concern for static flow systems is the potential build-up of contaminants during an exposure. With the addition of a mass flow controller and a needle valve, ExTEnD could be altered to allow for continuous flow operation in the future.

2.2. Testing

A large variety of different conditions were explored in order to improve the general understanding of the setup and optimise conditions for implantation. The range of parameters tested can be seen in Table 1. These included: stage bias, stage height, chamber pressure, electrode power and pulse off time. Although the use of a discharge plasma offered a simple way to produce a plasma, it did place restrictions on many of these parameters as conditions must be maintained in which it is possible to produce a discharge across the electrodes, whilst avoiding unwanted discharges elsewhere. This section presents a summary of conclusions from across the testing phase.

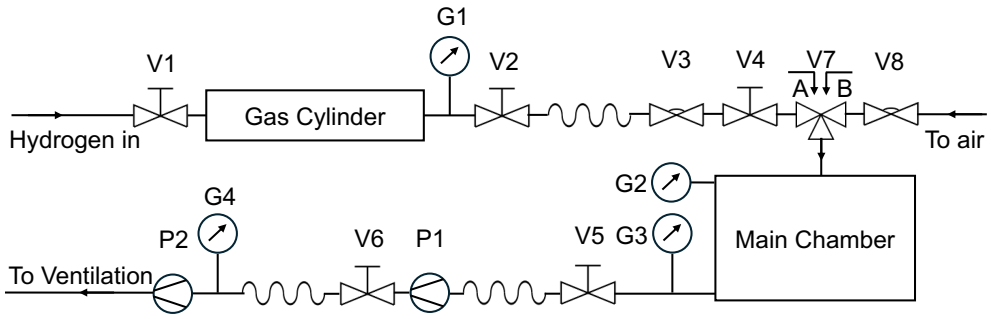

Figure 3: Piping and instrument diagram of the implanter setup. Valves are labelled 'V1' to 'V8', pressure gauges 'G1' to 'G4', and vacuum pumps 'P1' and 'P2'. V7 is a three-way valve which has two positions 'A' and 'B', gas flow of these positions are indicated below the V7 label. P1 was a turbo pump and P2 a dry scroll pump. G1 - Analogue gauge to measure gas cylinder pressure, G2 - Baratron (1 - 100 Torr) to monitor pressure during operation, G3 - Penning gauge for low pressure readings when pumping down, G4 - Pirani gauge to monitor scroll pump when pumping air.

Stage current was measured for each of the conditions tested. It was hoped the current required to maintain a setpoint bias would indicate the ion current incident on the stage. With no bias on the stage, the current reading gives the balance between electrons and ions hitting the stage, with a positive current reading indicating a greater number of electrons. Under some conditions, the stage can act like the grounded electrode, and electrons can stream from the negatively biased powered electrode directly to the stage resulting in high positive current readings. This is unlikely to occur with a moderate negative stage bias, as the potential difference will be greater between the electrodes than the powered electrode to the stage. Conversely, with a large stage bias that exceeds the stage-electrode breakdown voltage, electrons are emitted from the stage to the grounded electrode resulting in a large negative current measurement and the formation of a plasma discharge. Positive current measurements are a result of incident electrons, either from the plasma or from the powered electrode, whereas negative current readings are a result of incident positive ions or electrons emitted from the stage. For accurate fluence estimates, it is important that electron flow to and from the stage is avoided so the current measurement can be related to the number of incident ions.

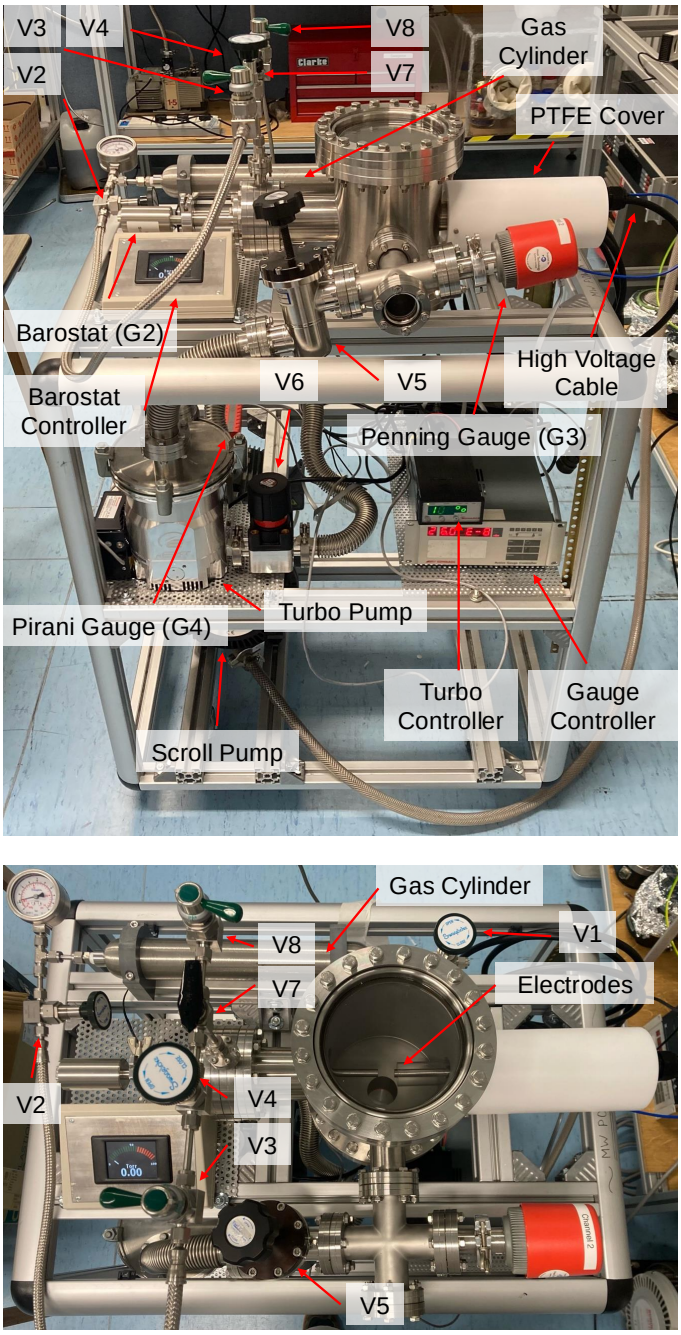

Figure 4: Full assembly as used for first plasma. Valve and gauge labels (V1-V8 and G2-G4 respectively) refer to Fig. 3. Sample stage assembly had not yet been fitted.

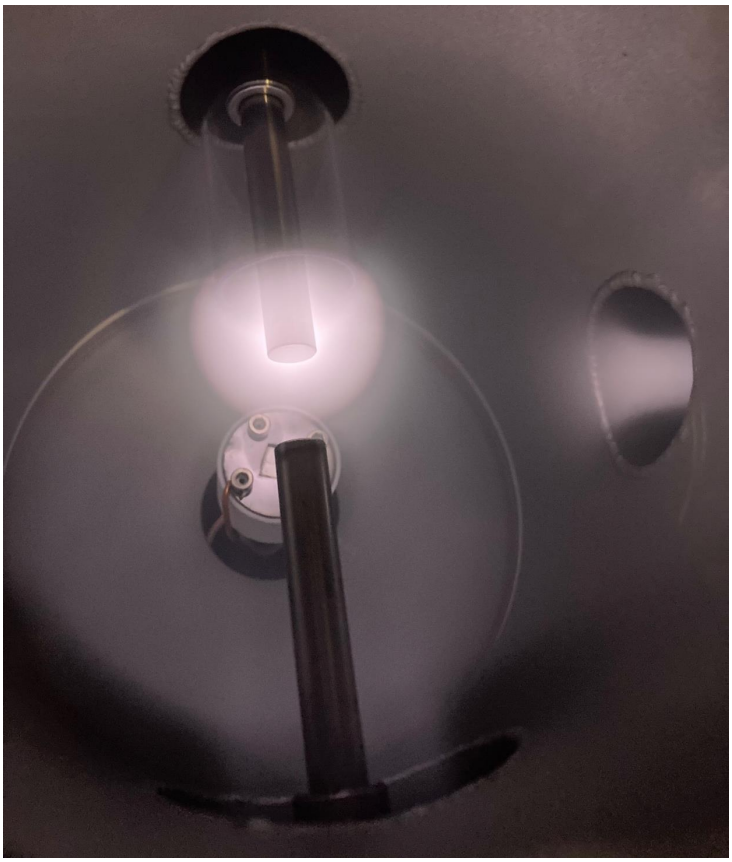

Figure 5: Image of an early hydrogen test plasma in ExTEnD, the pink colour is typical of a low pressure hydrogen plasma and is a result of the red and blue emissions of the Balmer series. Pressure: 0.1 Torr, Power: 50 W, Pulse frequency: 100 kHz, Pulse off time: 3 µs, Electrode-stage separation: 35 mm, Stage bias: 0 V.

2.2.1. Plasma Form

An early test plasma in ExTEnD can be seen in Fig. 5. At 0.1 Torr, a hemispherical plasma on the end of the powered electrode can be seen, as well as a secondary discharge along the internal of the 2.75" port that connects the main chamber to the Penning gauge and vacuum pumps. When increasing the pressure, the plasma is seen to increase in density, and condense around the electrodes, with the plasma sheath extending down the length of the powered cathode. The secondary discharge faded with increasing pressure and was no longer visible for pressures above 1 Torr. At pressures of 2 Torr and above with no stage bias, plasma discharge on the sample stage is visible, indicating a flow of electrons from the powered electrode. Applying a negative bias to the stage prior to striking the plasma decreased the potential difference between the cathode and the stage to below the breakdown voltage and prevented the discharge.

2.2.2. Power Supply Variables

A pulsed DC power supply with arcing suppression was used to create a discharge plasma across the electrodes and was run in constant power mode. In this setting, a voltage above the breakdown voltage is used and the supplied current is varied to meet the setpoint power. The voltage reading is time averaged across the pulses. Therefore, the pulse voltage, V_P, is given by

$$V_P = \frac{V_{avg}}{1 - f t_{off}}, \tag{1}$$

where V_{avg} is the voltage reading, f is the pulse frequency and t_{off} is the off time of the pulse. Standard operating conditions used a f of 100 kHz and a t_{off} of 3 µs, giving a pulsed voltage 1.43 times greater than the voltage reading.

Adjusting the pulse timings can be used to alter the stage current. Fig. 6 shows a linear relation between the time the power supply is on for and the stage current, suggesting t_{off} could be used to adjust ion current. However, it was unclear whether changes in pulse timings are truly reducing the ion flux or simply decreasing the time that the same high flux is being applied for (reducing the average flux). If the latter were true, the linear fit of Fig. 6 would be expected to pass through the origin (directly proportional), meaning halving the pulse length would result in half the stage current. However, the intercept of 0.13 mA means halving pulse length gives a stage current of lower than half the original value. For example, going from a time

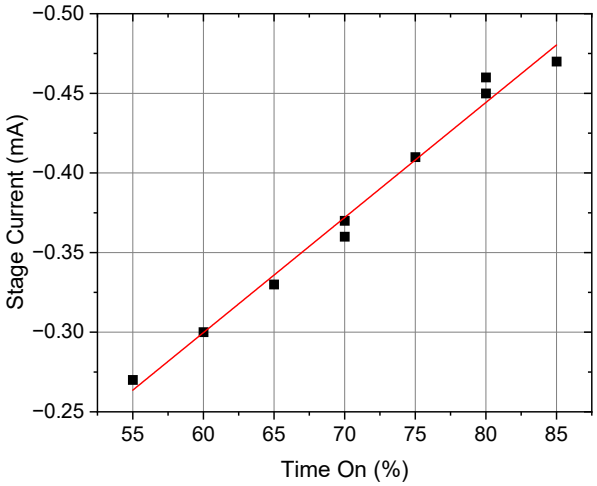

Figure 6: Stage current as a function of percentage of pulse time period for which the pulse was on. The pulse off time was varied between 1.5 – 4.5 µs in 0.5 µs increments, whilst the 100 kHz pulse frequency gave a time period of 10 µs. A linear fit has been applied giving a gradient of -0.072 ± 0.002 mA, an intercept of 0.13 ± 0.2 mA and an adjusted R^2 of 0.98. Pressure: 0.1 Torr, Power: 50 W, Pulse frequency: 100 kHz, Pulse off time: 3 µs, Electrode-stage separation: 65 mm, Stage Bias: -300 V.

on of 80% to 60% is a 25% reduction in pulse length but results in a 30% reduction in stage current. This lack of direct proportionality might suggest that longer pulse times increase the number of ions available during periods with the pulse off, meaning increasing or decreasing pulse length could be used to impact ion flux.

Varying plasma power can also be used to adjust stage current as shown in Fig. 7. For a pressure of 1 Torr, a plateau can be seen from 70 W and above for the three stage biases tested, this is comparable to ion flux measurements made with a Langmuir produce in other setups [12]. Current values scale with increasing stage bias. With a fixed stage bias (-250 V), the power curves vary form and magnitude with different pressures, with lower pressures appearing more linear and showing limited evidence of a plateau. At 5.2 Torr, the pressure is too high for notable current measurements, with the power supplied to the plasma having no impact on the 0 mA current reading. It was thought that varying power may offer a true change in ion flux, in contrast to pulse timings which may only impact the average flux.

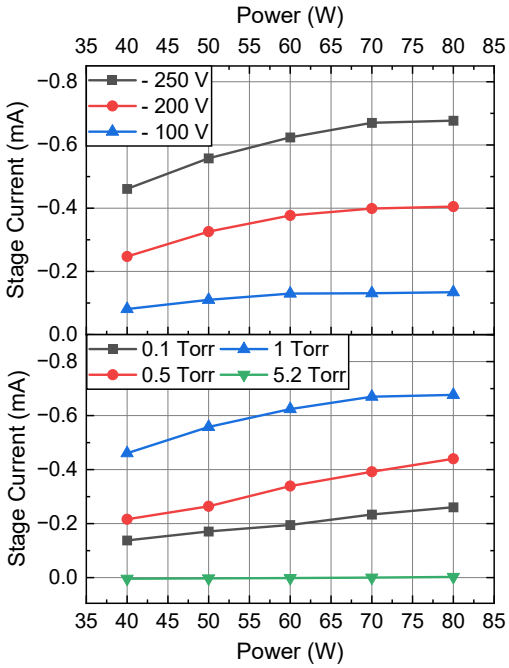

Figure 7: Stage current for varying plasma power. The top plot shows various bias voltages for a fixed pressure of 1 Torr, the bottom plot shows various pressures for a fixed bias of -250 V. Pulse frequency: 100 kHz, Pulse off time: 3 µs, Electrode-stage separation: 35 mm.

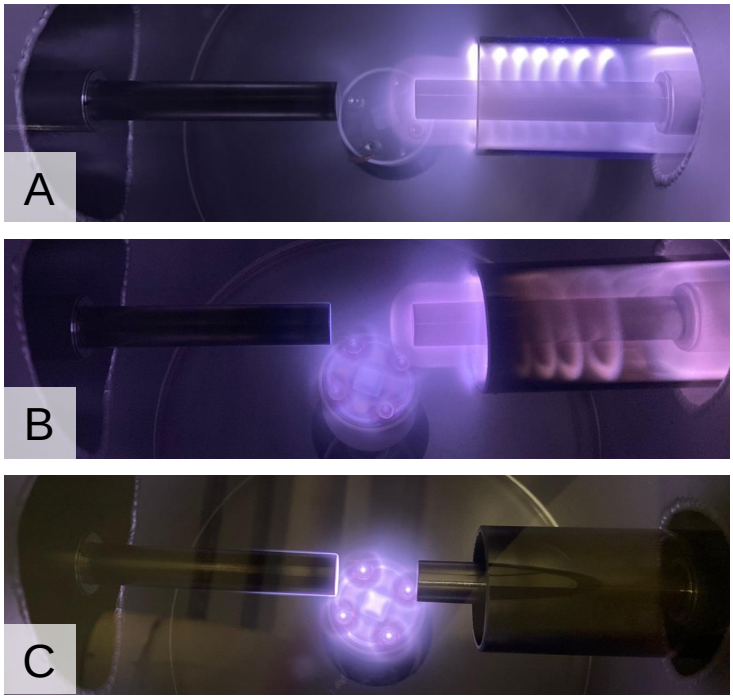

Figure 8: **A** - Desired operation, plasma discharge between electrodes (0 V stage bias), measured current corresponds to incident ions. **B** - Plasma discharge between electrodes and from the stage to the grounded electrode (-700 V stage bias). **C** - Plasma discharge from stage to grounded electrode with electrode power supply off (-700 V stage bias). Pressure: 1 Torr, Power: 50 W, Pulse frequency: 100 kHz, Pulse off time: 3 µs, Electrode-stage separation: 35 mm.

2.2.3. Sample Stage Variables

In order to determine operational conditions, stage bias ramps were performed at different pressures (for more information, see [11]). However, under some conditions, behaviour was observed that was suggestive electrode emission from the stage rather than the desired ion extraction. Sudden, step-wise, increases in stage current when increasing stage bias small amounts were observed, which are more indicative of exceeding a breakdown voltage than the smooth curve expected for ion extraction. This was confirmed with the observation of a discharge plasma on top of the stage (see Fig. 8).

The consequence of this behaviour on stage current is presented in Fig. 9. During desired operation (Fig. 9A), there is only electron flow between the electrodes, and a negative bias on the sample stage is used to extract positive

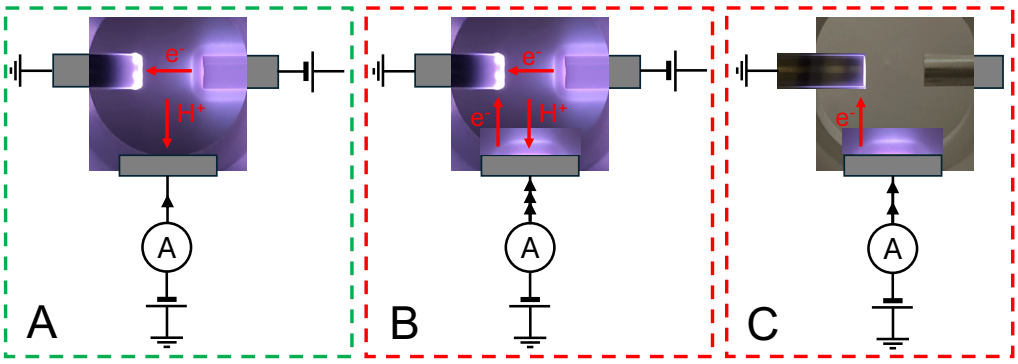

Figure 9: Simplified diagram of different sources of stage current, black arrows indicate the flow of electrons. **A** - Desired operation, discharge only between electrodes, measured current indicates incident ions. **B** - Discharge between electrodes and from the stage to the grounded electrode, measured current is the sum of ions incident on the surface and electrons leaving the stage. **C** - Discharge only present between grounded electrode and stage, measured current indicates electrons leaving the stage.

ions from the plasma. In this case, the ion energy is dictated by the stage bias and the stage current corresponds to the flux of incident ions on the surface. However, when the bias applied to the stage exceeds the breakdown voltage for those conditions, electrons stream from the negative stage to the grounded electrode, creating a Townsend avalanche and ionising hydrogen to form the plasma on the stage (as shown in Fig. 9B). Here, the stage is acting in a similar manner to the negatively biased powered electrode. When this occurs, the current reading no longer corresponds to the flux of ions hitting the stage but is a combination of electron emission and ions incident on the stage, and both ion flux and energy becomes unclear. With the electrode power supply off and a sufficient stage bias, only the stage discharge is present, and current measurements correspond to electrons leaving the stage (Fig. 9C). As the powered electrode is either negatively biased or isolated, electrons will always preferentially flow to the grounded electrode. Evidence of this can be seen in Fig. 8C, where plasma can only be seen on the stage and around the underside of the grounded electrode.

When performing a bias ramp, the resulting IV curve is a combination of ion flux on the stage, and loss of electrons from the stage. In order to perform and measure ion extraction at a set energy, the stage-electrode discharge must be avoided, and conditions must be determined in which the electron flow between the stage and electrodes is negligible. The variables

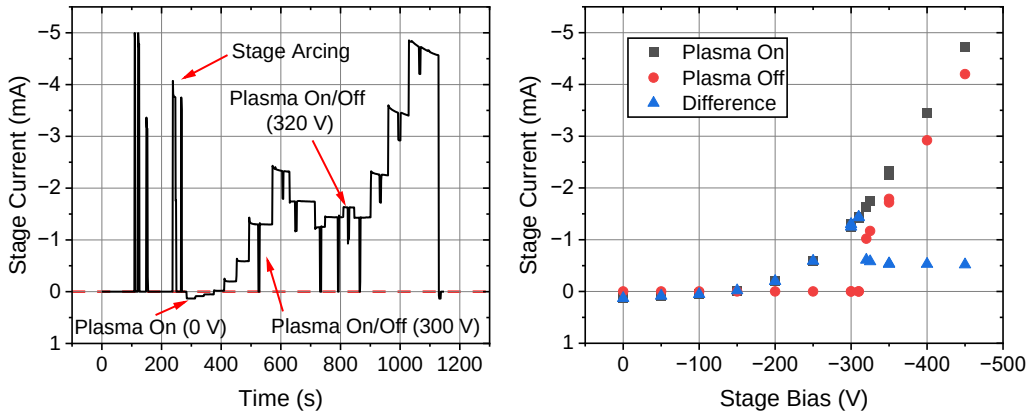

Figure 10: Current measurements taken to measure breakdown voltage between the stage and grounded electrode. The figure on the left shows current with respect to time during this test. Initial spikes were a result of electron emission from the stage to the grounded electrode with the electrode power supply off. Following this, discrete steps in current are a result of changes in stage bias. Sudden drops in current are when the electrode power supply was turned off and on again. The figure on the right gives the measured stage current with the electrode power supply on and off, as well as the difference between them, for various stage biases. Pressure: 1 Torr, Power: 50 W, Pulse frequency: 100 kHz, Pulse off time: 3 µs, Electrode-stage separation: 65 mm.

which influence the stage-electrode discharge the most are chamber pressure and stage-electrode separation. As such, bias ramps were performed at four different stage heights (corresponding to stage-electrode separation of 25, 35, 50 and 65 mm) at six pressures (0.1, 0.5, 1, 2, 5, 10 Torr). In an attempt to determine at what stage bias the stage-electrode discharge forms, the electrode power supply was turned off and on at selected biases. With a negative stage bias and the electrode power supply off, any stage current must be a result of electrons flowing from the stage to the grounded electrode.

An example of these tests can be seen in Fig. 10. Current measurement with respect to time during the tests can be seen on the left, whilst the current measurement at each stage bias is presented on the right. The initial peaks on the current-time plot were a result the stage-electrode discharge with the electrode power supply off. This was done to get an estimate of the breakdown voltage prior to the bias ramp. The first off/on of the electrode power supply can be seen at around 500 s (-300 V bias). Here, the stage current returns to 0 mA when the plasma is off, indicating no electron flow is present with the plasma off. The following bias step (560 s, -350 V) shows a decrease to a non-zero current measurement, indicating electron flow from the stage to the grounded electrode with the plasma off. The lowest voltage that this was true for is -320 V. For voltages higher than this, the reduction in current is consistently around 0.5 mA, as shown in the difference between plasma on and off in Fig. 10.

As the stage current is thought to be a combination of contributions from electron emission and incident ions, the difference between current measurements with the plasma on and off could be used to indicate ion current. However, there are clearly limitations to this simplification, as it relies on ion and discharge currents being independent of one another. Although it can be said with some certainty that the plasma off current is solely a result of electron flow to the grounded electrode, it cannot be said that this contribution remains the same with the plasma on. There is evidence of this at biases just below the stage-electrode breakdown voltage. For some conditions, the plasma off current was 0 mA but a stage discharge was present with the electrode plasma on. This indicates that, under these conditions, the current contribution from the discharge was not equivalent with the plasma on and off. Similarly, at this bias, the difference in current was greater than the constant value observed for biases beyond the breakdown voltage. These observations suggest the presence of free ions and electrons are enhancing the stage-electrode discharge, allowing it to occur despite the stage bias being

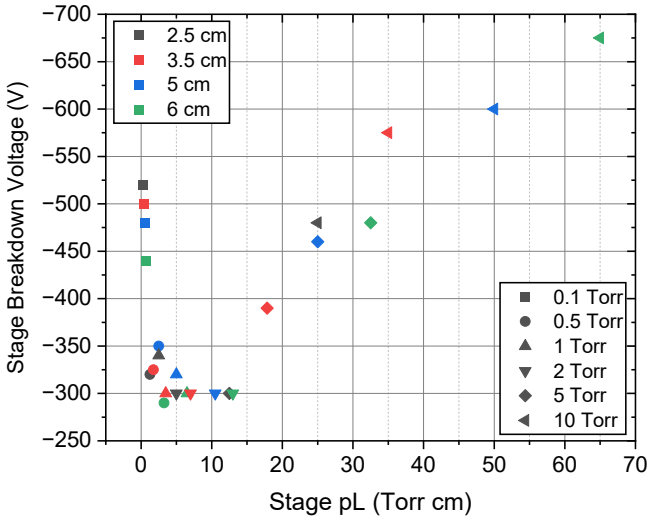

Figure 11: Breakdown voltage between the sample stage and grounded electrode for varying pressure (indicated by different symbols) and stage-electrode separation (indicated by different colours). Power: 50 W, Pulse frequency: 100 kHz, Pulse off time: 3 µs.

below the breakdown voltage.

The constant value observed in the current difference of Fig. 10 could be an indication of an ion saturation current as observed in IV curves of Langmuir probes. However, this constant value did not follow trends that would be expected for ion current measurements (decreasing with increasing pressure or separation). Furthermore, as the presence of the electrode plasma enhances the stage-electrode discharge, it is challenging to conclude with any confidence what this is a result of. Beyond the breakdown voltage the contribution from electron flow is effectively unknown, as it was concluded that discharge current is unlikely to be equivalent with the plasma on and off. Therefore, for effective ion extraction of known energy and measured flux, a bias beyond the breakdown voltage cannot be used and conditions must be selected that ensure the stage-electrode electron flow is not present with the plasma on.

Fig. 11 shows the highest voltage at which the stage current returned to 0 mA for pressures up to and including 2 Torr. For pressures of 5 Torr or more, the bias supply would suddenly trip at high bias - indicating a stage current

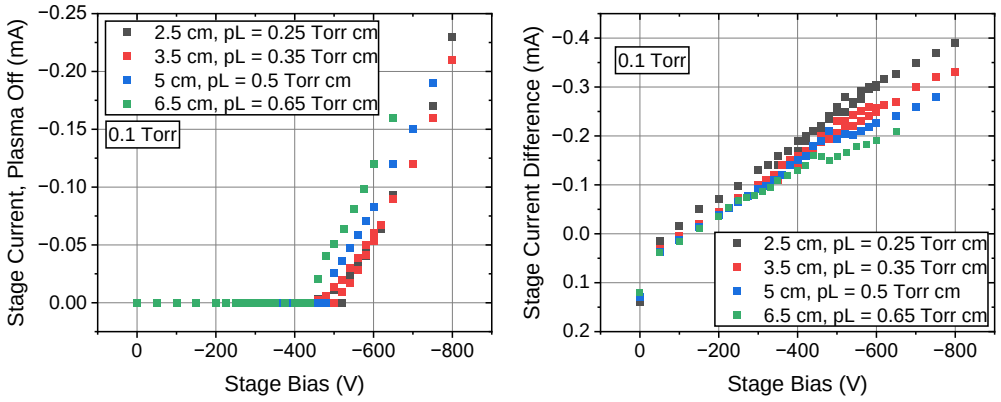

Figure 12: The difference between stage current with the stage current with the plasma off (left) and the electrode plasma on and off (right) and for varying stage biases. The stage-electrode separation and resulting pL value is indicated in the legend. Pressure: 0.1 Torr, Power: 50 W, Pulse frequency: 100 kHz, Pulse off time: 3 µs.

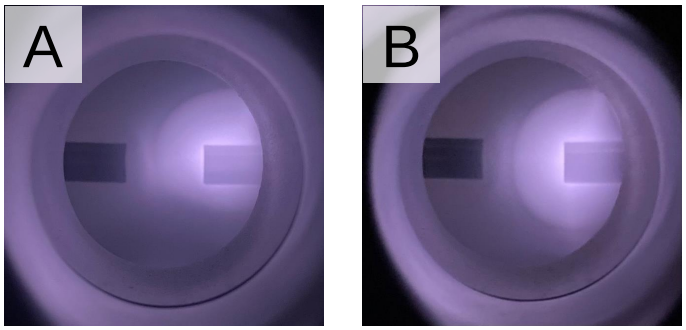

Figure 13: The shortest stage-electrode separation of 25 mm (**A**) distorts the form of the plasma, whereas a separation of 35 mm (**B**) does not. Pressure: 0.1 Torr, Power: 50 W, Pulse frequency: 100 kHz, Pulse off time: 3 µs, Stage bias: -400 V.

in excess of -10 mA and significant electron flow between the stage and grounded electrode. As no negative current readings were observed before this point, Fig. 11 presents the highest stage bias at which no trip occurred for $p \geq 5$ Torr. Although not a typical measure of breakdown voltage, the shape of this curve bears a resemblance to a Paschen curve, with a minimum in breakdown voltage occurring at a pL of 5–10 Torr cm. This minimum is slightly higher than the 1 Torr cm determined via a more standard manner [13]. Measurements at 0.1 Torr are of particular interest. As can be seen in Fig. 11, this pressure gives pL values below the Paschen minimum and therefore minimises the likelihood of the stage-electrode discharge occurring. Furthermore, ion current would be expected to drop off with both p and L, so minimising pressure should maximise the extracted ion current. As this is in contrast to discharge current which increases with pL below the Paschen minimum, meaning the two current sources can be separated by varying pL.

Fig. 12 shows the stage current with the plasma off, and the difference in stage current with the plasma on and off, for a pressure of 0.1 Torr. As discussed, any measured stage current with the plasma off must be a result of stage-electrode electron flow. As the pL values for these datasets are all below the Paschen minimum, increasing pL results in a lower breakdown voltage and a larger current. In contrast, the difference in stage current decreases with increasing pL. The stage current with the plasma on is thought to be a combination of charge contributions from incident ions and electron emission from the stage. Although there are limitations, the difference between plasma on current and plasma off current could be used to indicate the ion current contribution[1]. The difference in current behaves in the same expected manner as ion current and decreases with L, whilst the plasma off current, which must be a measure of lost electrons, increases with L. Therefore, it was concluded that below the breakdown voltage at these low pL values, the rate of electron emission from the stage is minimal and stage current can be used to measure incident ions on the stage. At higher pressures, the lower breakdown voltage creates more restrictions on possible operating conditions, and it becomes more challenging to differentiate between stage emission and ion extraction regimes. At pressures of 5 Torr and above, the applied bias

[1]Under these conditions, the current contribution from stage-electrode discharge when present appears to be minimal, and below the breakdown voltage the difference in current is simply the measured stage current.

Table 2: Standard operating conditions for ExTEnD.

ExTEnD Exposure Conditions	
Pressure	0.1 Torr
Stage-Electrode Separation	35 mm
Stage Bias	-400 V
Electrode Power	50 W
Pulse t_{off}	0.3 µs
Exposure Time	Approx. 30 minutes
Gas	Deuterium

had a minimal impact on the measured current (which consistently read low positive values) until a sudden arc would form at the breakdown voltage. This behaviour suggests no ion current could be measured at higher pressures due to the increased scattering effects, and any negative stage current measured is solely a result of electron emission from the stage.

Based on these conclusions, a stage-electrode separation of 35 mm was selected. Although a shorter separation could help minimise the risk of stage discharge further, at 25 mm, the stage began to distort the form of the plasma as shown in Fig. 13. Standard operational conditions for ExTEnD can be seen in Table 2.

2.2.4. Fluence Estimation

Assuming a uniform beam distribution, and that stage current is a result of ions incident on the sample stage, the total fluence of deuterium incident on a sample during an exposure can be approximately determined. Integrating the stage current, $I(t)$ over the time t, can be used to estimate the charge accumulated on the sample,

$$Q_{Sample} = \frac{A_0}{A_1} \int I(t)dt, \tag{2}$$

the fluence,

$$f = \frac{\alpha}{eA_1} \int I(t)dt, \tag{3}$$

the average flux,

$$F_{avg} = \frac{\alpha}{eA_1 t_0} \int I(t)dt, \tag{4}$$

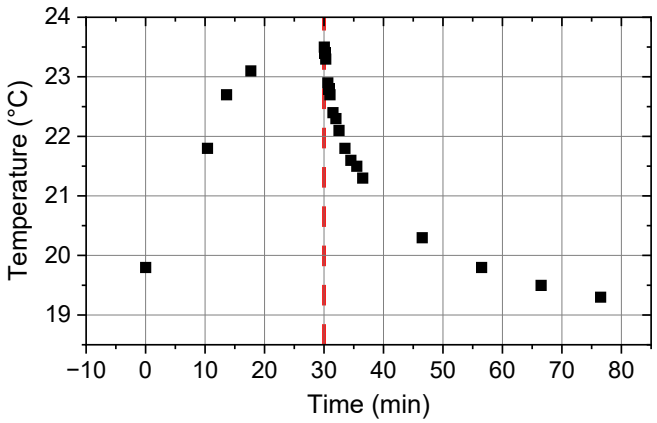

Figure 14: Sample stage temperature during exposure to plasma and when cooling down. The plasma and stage bias were both on for the first 30 mins, before being turned off and left to cool for time > 30 mins.

and the instantaneous flux,

$$F = \frac{\alpha I}{eA_1}. \tag{5}$$

Here, A_0 and A_1 are the exposure area and stage area respectively, α is the average deuterium cluster size (taken to be 2.96 D [7]), e is the charge of each ion and t_0 is the exposure time. Using this calculation, a 0.1 mA stage current corresponds to a stage flux of order 10^{18} m^{-2} s^{-1}.

2.2.5. Temperature Measurement

Temperature is known to have a significant impact on the uptake of molecules into a material. As ExTEnD has no temperature controlled stage, a one-time temperature measurement was taken. To perform the measurement, the secondary viewport was replaced with a thermocouple feedthrough, and a k-type thermocouple connected, with the probe secured directly to the stage. The temperature measurement was carried out under standard operational conditions (see Table 2). To ensure this stage temperature measurement was a close approximation to sample temperature, no sample was present, meaning the full surface of the stage was exposed.

Fig. 14 shows the stage temperature during a 30 minute exposure followed by a cool down period. The maximum temperature measured was 23.5 °C. Judging by the plateau in temperature, it seems reasonable to claim the

sample is not expected to exceed a temperature of 25 °C, even for longer runs.

3. Impact of ion flux on deuterium retention in Eurofer - a preliminary study

3.1. Method

For this preliminary study, deuterium ion exposures were conducted on reduced activation ferritic-martensitic Eurofer steel with the nominal chemical composition (wt.%): Fe-0.1C-9Cr-1.1W-0.45Mn-0.2V-0.12Ta. The material was supplied in the as-rolled condition as a 4 mm thick plate. Five equivalent samples with dimensions of 10 × 10 × 1 mm^3 were extracted from the plate using electrical discharge machining (EDM). All sample surfaces were sequentially ground with silicon carbide (SiC) papers up to 1200 grit. The surface exposed to deuterium was subsequently mirror-polished using diamond suspensions with decreasing particle sizes, down to 0.25 µm.

Four of the Eurofer samples were exposed in ExTEnD to different deuterium ion fluxes, whilst the final sample remained unexposed. Post exposure, the deuterium and hydrogen retention was evaluated using thermal desorption spectroscopy (TDS). Eurofer was developed as a structural material for fusion applications [14], and was selected for this study as a fusion-relevant metal which had been tested in an established setup under similar conditions [6]. Sample preparation, exposure conditions, and TDS procedure followed [6] as closely as possible to evaluate this new setup. Flux and fluence were estimated from the stage current using Eq. 4 and Eq. 3 respectively. Exposures were carried out at ambient temperature, at an estimated fluence of 1.0×10^{22} m^{-2}. The most notable difference between the exposures carried out here and in [6] was the flux. Under standard operating conditions, ExTEnD has an ion flux roughly an order of magnitude higher than DELPHI - the facility used in [6]. The flux in ExTEnD can be adjusted in two ways: the pulse timings and the plasma power. As discussed in section 2.2, varying plasma power is thought to offer a true adjustment in flux, whereas it was unclear whether changes to pulse timings only altered the average flux.

A summary of exposure conditions can be seen in Table 3. The intention for these experiments was to test four samples at one of three different fluxes: one sample at high flux, one sample at a low flux, and two samples at a roughly equivalent medium flux but with different t_{off} and power values. Of the two mid flux samples, the higher power sample (sample C) was

Table 3: Measured variables for four samples exposed at different fluxes in ExTEnD. 'Pulse Power' and 'Pulse Flux' are scaled in a similar manner to Eq. 1 to account for pulse timings.

Sample	**A**	**B**	**C**	**D**
Stage Bias (-V)	400	400	400	400
Electrode Power (W)	70	40	50	30
Pulse Power (W)	77	44	91	55
Electrode Voltage (-V)	644	507	247	180
Electrode Pulse Voltage (-V)	716	563	449	327
t_{off} (µs)	1	1	4.5	4.5
Estimated Average Flux ($\times 10^{18}$ $m^{-2}s^{-1}$)	9.67	6.39	8.71	2.33
Estimated Pulse Flux ($\times 10^{18}$ $m^{-2}s^{-1}$)	10.74	7.10	15.84	4.25
Exposure time (minutes:seconds)	17:33	26:27	19:33	71:28
Estimated Fluence ($\times 10^{22}$ m^{-2})	1.02	1.01	1.02	1.00

tested first, with a long t_{off} to reduce the power. For the other mid flux sample (sample B), the t_{off} was reduced to the minimum feasible value and the smallest decrease in power (10 W) in an attempt to match the flux of sample C. Despite this, the flux for sample B remained lower than sample C. Although this could suggest variations in power offer more course adjustment, it is worth noting there is a notable variation day-to-day in measured ion currents, even for equivalent conditions. For sample B, the power was briefly increased to 50 W and, although an increase in current was seen, it did not reach the same ion currents as sample C despite the shorter t_{off}.

Post exposure, TDS measurements were performed using a Hiden Analytical Ltd Type 640100 TPD workstation workstation available at the Department of Engineering Science, University of Oxford [15]. The TDS procedure of [6] was also reproduced. Between exposure and measurement there was a gap of approximately 1 day (28 hrs in this study), and in both measurements the sample stage was heated from room temperature to 1273 K at a ramp rate of 10 K min^{-1} and held at the maximum temperature for one-hour. An AlN layer was placed between the heater and the sample as is commonplace in TDS measurements (although it is unclear whether one was used in [6]),

meaning a temperature correction was required to account for the slower heat transfer to the sample. The correction was determined by measuring argon desorption from silicon, which displays a narrow peak at a known temperature. Background counts were measured for this temperature profile and removed from final results. Leak calibration tests were performed with both H_2 and D_2 to obtain calibration factors, with the calibration factor for HD taken to be the average between the two.

Alongside the four exposed samples tested, two unexposed samples were also measured for reference. These samples were prepared in the same manner as the other samples and followed the same TDS measurement procedure. Both samples produced near identical results, so only one sample has been presented in the results. For all samples, a base pressure of 10^{-8} Torr was achieved pumping down overnight, suggesting the use of a static gas volume has not introduced excessive contaminants to the system.

3.2. Retention Results and Discussion

Desorption peaks from Eurofer samples align well with other deuterium retention experiments, including [6]. There have been a significant number of studies exploring hydrogen isotope retention in Eurofer with TDS, with a wide variety of techniques used to introduce hydrogen into the metal. These methods include ion implantation [4, 5, 6, 16, 17, 18, 19, 20, 21], exposure to a glow discharge [8, 22, 23], plasma submersion [24], electrochemical charging [9, 25] and gas permeation [10, 26, 27]. Even when only ion implantation is considered, exposure temperature, flux, fluence and ion energy can impact uptake of hydrogen, whilst the temperature ramp rate and even the time between exposure and TDS measurement will play a role in the desorption of hydrogen. Despite this, similarities are observed between the TDS spectra of these studies. All data seems to present with some, if not all, of three desorption peaks, referred to as peaks 1–3. The most commonly observed peak was the low temperature peak (peak 1), reported in the 130–220 °C range, [9, 16, 17, 19, 22, 25, 27] in good agreement with the 167 °C peak seen here. Furthermore, this is in very good agreement with the 175 °C seen in [6] from which the TDS procedure had been replicated. Some studies have also reported the presence of two higher temperature peaks [5, 6, 10, 18, 21, 26], which are likely to correspond to the 420 and 630 °C peaks (peaks 2 and 3 respectively) seen in this data. Typically, these peaks are diminished compared to the low temperature peak [6], but are still required for accurate fitting of desorption spectra [10, 26]. Furthermore, some have

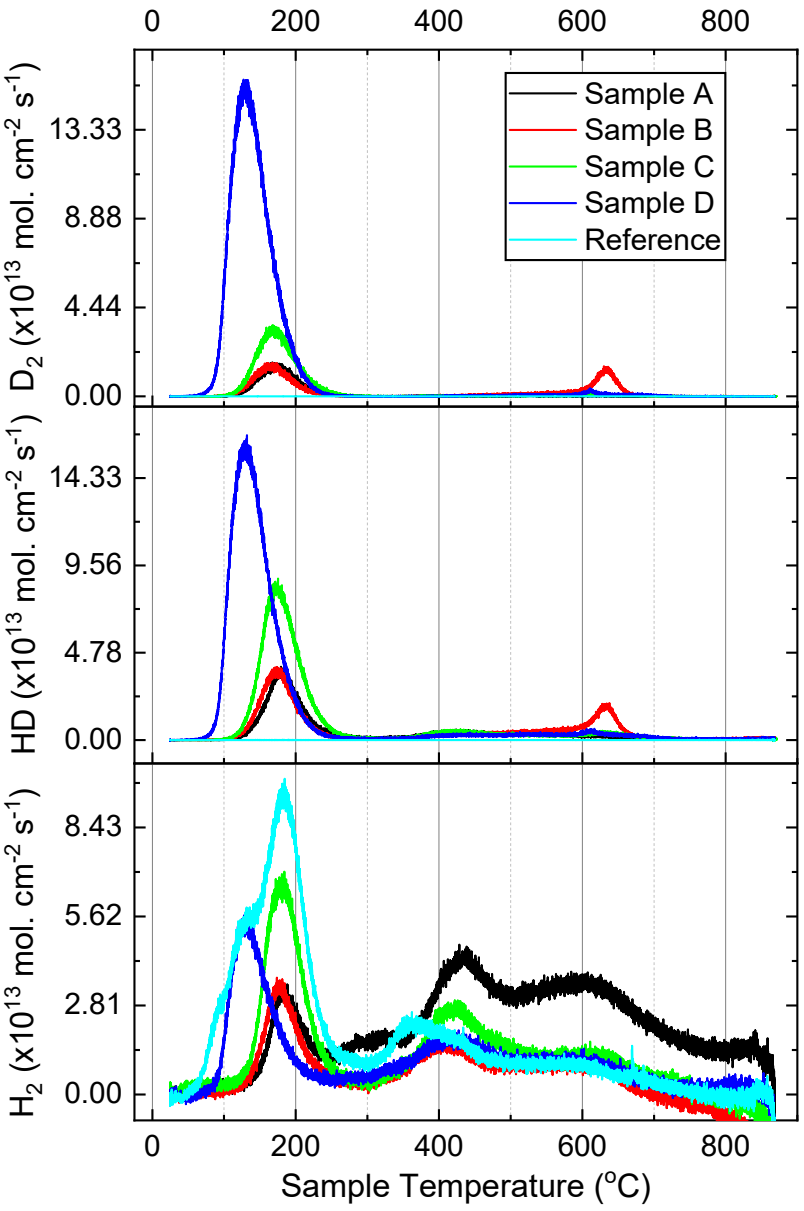

Figure 15: Thermal desorption spectroscopy (TDS) measurements for four Eurofer samples exposed to deuterium ions under different conditions. An equivalent but unexposed reference sample was also measured. Masses 2, 3 and 4 were attributed to H_2, HD and D_2 respectively, counts were calibrated and scaled by exposure area to give molecules per area and plotted against the sample's temperature, which was calculated by applying a temperature correction to the stage temperature.

Table 4: Calibrated total counts from TDS data for Eurofer samples exposed in ExTEnD at different fluxes and a fluence of 1.0×10^{18} cm^{-2}. Retention values have been scaled by exposure area (0.64 cm^2) rather than sample size (1 cm^2).

Sample	HD ($\times 10^{16}$cm^{-2})	D_2 ($\times 10^{16}$cm^{-2})	Total D ($\times 10^{16}$cm^{-2})
A	2.41	0.735	3.88
B	3.05	1.20	5.43
C	4.63	1.65	7.92
D	8.29	7.21	22.70

observed comparable retention in peaks 1 and 3 [26] (as is the case for sample B), and others have suggested fluence could play a role in the ratio between the peaks [18]. Some studies only observed higher temperature peaks with peak 1 absent from spectra all together [5, 21]. Although modelling of TDS experiments [28] can help to characterise trapping sites, across the literature there are no clear trends between exposure conditions and which peaks are present. The high native hydrogen content of the reference sample highlights the presence of stable trapping sites within these samples. Desorption at high temperatures is likely a result of trapping in vacancies or other defects leading to very stable trap sites.

The most obvious difference between the samples is the high retention of sample D which is almost three times higher than the next closest sample (see Table 4). The only variable that correlates with the total retention in each sample is the electrode voltage, which decreases from sample A to D whilst retention increases. The only way the electrode voltage could influence retention measurements would be if the varying voltage was impacting the ion current measurement, leading to inaccurate flux estimation and different fluences between the samples. However, this is unlikely, as the maximum potential difference between the stage and powered electrode is around 316 V (for sample A) which is below the breakdown voltage of 500 V for these conditions (see Fig. 11) so significant electron flow from/to the powered electrode is not expected. Instead, it is thought that the greater retention of sample D was a result of the longer exposure time. The fast diffusion of hydrogen isotopes in metals means the exposure time can play a significant role on hydrogen uptake depending on the technique used. For example, in electrochemical hydrogen loading, the surface becomes completely saturated with hydrogen which gradually diffuses into the sample and retention in-

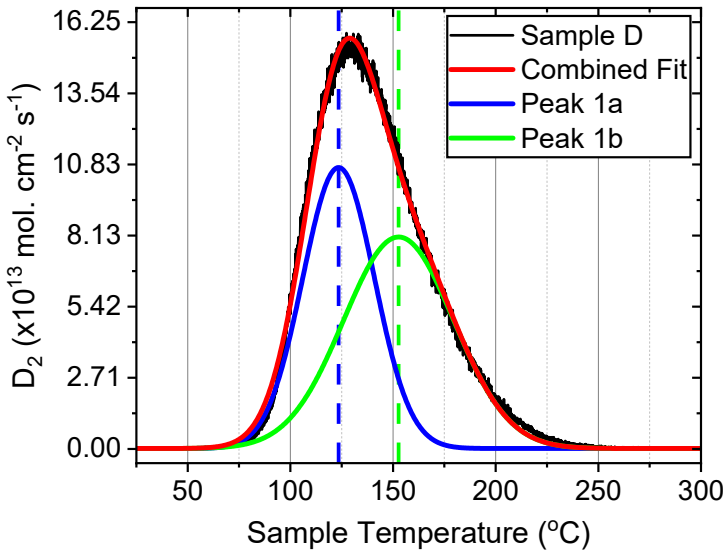

Figure 16: Gaussian deconvolution of low temperature D_2 peak of sample D. Counts were calibrated and scaled by exposure area to give molecules per area. The 2 peak fit gave an adjusted R^2 of 0.997. 'Peak 1a' and 'Peak 1b' show the 2 peak deconvolution, with dashed lines indicating the peak positions of 123.5 °C and 152.7 °C.

creases with time (up to a saturation point). In this work, 400 eV deuterium clusters are likely to penetrate small distances into the material. The shallow depth of the low-energy ions will mean that saturation of a thin layer would be expected. In this scenario, the surface concentration during exposure would be similar across the different exposures, and total retention would be dominated by the exposure time. For longer exposures, deuterium is can diffuse from the saturated layer deeper in the material, allowing more deuterium into this top layer. Although no general trend between exposure time and retention was observed, the exposure times of samples A, B and C were all comparable, and different exposure conditions likely resulted in some fluctuations of retained deuterium. Sample D however had a much longer exposure time and subsequently much greater retention. Generally, the retention values determined of 10^{19}-10^{20} m^{-2} are comparable to those of other studies [5, 16, 18, 20, 21].

Peak 1 in sample D also appears to have shifted 40 °C lower than the other samples. However, it seems that peak 1 actually consists of two smaller

peaks (1a and 1b) at similar temperatures, meaning the shift is less significant than it initially appears. This can clearly be seen in the H_2 spectra of the reference sample, where a dominant peak at 185°C is observed with a shoulder at 130°C. On closer inspection, peak 1 of sample D appears less symmetric than the other samples, and deconvolutes well into two peaks as shown in Fig. 16. Therefore, it is believed that the apparent shift in peak 1 for sample D is actually a result of a more prominent peak 1a. Both peaks 1a and 1b must be highly stable binding sites, as they remain prominent in the unexposed reference sample. From this data alone, it is challenging to conclude what has caused this change in peak 1. It is possible that some physical difference between sample D and the other samples is present as a result of the different exposure conditions. This could have impacted which sites are occupied by both deuterium and hydrogen and changed the form of peak 1. Although peak 1a aligns well with the shoulder peak of the reference H_2 spectrum, the second peak of this spectrum is around 30 °C higher than peak 1b. Others have suggested shifts in peaks are a result of damage to the sample [6], further suggesting some physical difference between sample D and the other samples may be present post-exposure.

The other notable difference between the spectra is the prominence of peak 3 in sample B. The high temperature of this peak implies desorption from very stable trapping sites (such as vacancies, voids or other defects) and suggests the surface of this sample may have been damaged during exposure. Although other samples presented some evidence of this peak, this was the only sample which gave counts similar to that of peak 1 in D_2 counts. From these results, there is no clear reason as to why exposure conditions for this sample would result in additional damage compared to the other samples. At temperatures below 600 °C, spectra of sample A and B are remarkably similar. Both samples used the longer pulse, but sample B was at a lower power (40 W compared to 70 W). It is unlikely the presence of the high temperature peak is a result of the lower power as sample D (30 W) did not present this peak. Similarly, sample B had a lower flux than both A and C but not of D, meaning flux is unlikely to be the determining factor. Others [18] concluded the ratio between the high and low temperature peaks was impacted by fluence, with the traps corresponding to the first peak filling up last and the high temperature peak dominating at low fluence. Although this explanation aligns well with the data presented in [18], far lower fluences have failed to present the high temperature peak (in this work and much of the work referenced in this section). Again, differences in this paper and

the work of others are numerous, making it challenging to directly compare results.

Generally, the flux and fluence are thought to impact the surface interaction, and the formation of defects that result in deuterium trapping [29, 30]. Because of this surface interaction, the impact flux has is highly dependent on the material [31]. However, in this work, no clear trends were observed in both flux and pulse flux. These observations are likely a result of surface saturation leading to comparable deuterium concentrations during the exposures, and total retention being mostly impacted by exposure time. Testing notably lower fluxes may result in lower surface concentrations during exposure - allowing flux to have a more obvious impact on total retention. Similarly, using significantly higher fluxes may increase damage sustained to the surface and impact retention mechanisms in this way. There was nothing to suggest the manner in which flux was varied (pulse timings or plasma power) impacted results, implying both of these could be used to adjust the flux and account for the day to day variations. Future work could look to vary fluence at a consistent flux to verify whether surface saturation is likely.

4. Conclusions

A new setup capable of performing low energy hydrogen/deuterium implantations at a controllable ion energy and measurable flux has been assembled and tested. Under standard operating conditions, ExTEnD can perform ion exposures across an 8×8 mm^2 area at room temperature, with ion energies up to 400 eV (135 eV per D) and a flux of approximately 4×10^{18} m^{-2} s^{-1}. Use of a pulsed DC plasma aided the simplicity and cost of the setup, although it added restrictions on the exposure conditions possible. Through careful selection of operational conditions, it was possible to find settings which meant stage current could be used as an approximation for flux, and stage bias could be used to dictate ion energy.

Retention measurements of Eurofer samples were in good agreement with a diverse selection of similar studies. Evidence of the three peaks commonly seen in Eurofer samples was observed, although exposure conditions could not be related to the absence of some peaks in the literature or in the data presented here. Additional and repeated measurements would be required before more definitive conclusions can be drawn. Similarly, there was no clear indications that power or pulse timings couldn't be used to vary flux, but more testing would be required to ensure these could be used to account

for variations in flux to maintain repeatability. Three of the samples tested gave comparable results, whilst the lowest flux sample presented a clear increase in retention. This observation was thought to be a result of similar surface concentrations during the different exposures, meaning the increased exposure time of the low flux sample permitted more deuterium to diffuse into it.

Acknowledgements

The authors would like to thank D. C. Fairclough and O. Tarvainen (UKRI Science and Technology Facilities Council, UK) for their advice and guidance relating to ion extraction and interpretation of results from testing. E. Martínez-Pañeda acknowledges financial support from UKRI's Future Leaders Fellowship programme (grant MR/V024124/1).

References

[1] K. O. E. Henriksson, K. Nordlund, A. Krasheninnikov and J. Keinonen, The depths of hydrogen and helium bubbles in tungsten: A comparison, Fusion Sci. Technol. 50:43–57, 2006

[2] M. R. Gilbert, Ž. Zacharauskas, P. Almond, N. Scot-Mearns, S. Reynolds *et al.*, Fusion waste requirements for tritium control: Perspectives and current research, Fusion Eng. Des. 202:114296, 2024

[3] D. Matveev, D. Douai, T. Wauters, A. Widdowson, I. Jepu *et al.*, Tritium removal from JET-ILW after T and D–T experimental campaigns, Nucl. Fusion 63:112014, 2023

[4] Z. Harutyunyan, Yu. Gasparyan, S. Ryabtsev, V. Efimov, O. Ogorodnikova, A. Pisarev, S. Kanashenko, Deuterium trapping in the subsurface layer of tungsten pre-irradiated with helium ions, J. Nucl. Mater., 548:152848, 2021.

[5] R. Arredondo, M. Balden, T. Schwarz-Selinger, T. Höschen, T. Dürbeck *et al.*, Comparison experiment on the sputtering of EUROFER, RUSFER and CLAM steels by deuterium ions, Nucl. Mater. Energy, 30:101118, 2022.

[6] A. Hollingsworth, M. Y. Lavrentiev, R. Watkins, A. C. Davies, S. Davies *et al.*, Comparative study of deuterium retention in irradiated Eurofer and Fe-Cr from a new ion implantation materials facility, Nucl. Fusion, 60:016024, 2020

[7] A. Manhard, T. Schwarz-Selinger and W. Jacob, Quantification of the deuterium ion fluxes from a plasma source, Plasma Sources Sci. T., 20:015010, 2011.

[8] E. Malitckii, Y. Yagodzinskyy and H. Hänninen, Hydrogen charging process instrument, Fusion Eng. Des, 100:142–145, 2015

[9] Y. Yagodzinskyy, E. Malitckii, M. Ganchenkova, S. Binyukova, O. Emelyanova *et al.*, Hydrogen effects on tensile properties of EUROFER 97 and ODS-EUROFER steels, J. Nucl. Mater., 444:435–440, 2014.

[10] F. Montupet-Leblond, L. Corso, M. Payet, R. Delaporte-Mathurin, E. Bernard *et al.*, Permeation and trapping of hydrogen in Eurofer97, Nucl. Mater. Energy, 29:101062, 2021.

[11] J. A. Pittard, Retention of hydrogen isotopes in diamond for applications in fusion energy - PhD Thesis, University of Bristol Department of Physics, 2025.

[12] D. Gahan, S. Daniels, C. Hayden, P. Scullin, D. O'Sullivan *et al.*, Ion energy distribution measurements in RF and pulsed DC plasma discharges Plasma Sources Sci. Technol., 21:024004, 2012.

[13] I. Korolov and Z. Donkó, Breakdown in hydrogen and deuterium gases in static and radio-frequency fields, Phys. Plasmas, 22:093501, 2015.

[14] R. Lindau, A. Möslang, M. Rieth, M. Klimiankou, E. Materna-Morris *et al.*, Present development status of EUROFER and ODS-EUROFER for application in blanket concepts, Fusion Eng. Des., 75–79:989–996, 2005.

[15] A. Zafra, Z. Harris, E. Korec and E. Martínez-Pañeda, On the relative efficacy of electropermeation and isothermal desorption approaches for measuring hydrogen diffusivity, Int. J. Hydrogen Energy, 48(3):1218—1233, 2023.

[16] A. Theodorou, K. Schmid, T. Schwarz-Selinger, Annealing of hydrogen trap sites in displacement-damaged EUROFER, Nucl. Mater. Energy, 38:101595, 2024.

[17] O. V. Ogorodnikova, Z. Harutyunyan, Yu. Gasparyan, V. Efimov, Helium and deuterium retention in Eurofer97 under sequential irradiation at low fluxes, J. Nucl. Mater., 568:153871, 2022.

[18] Y. Martynova, M. Freisinger, A. Kreter, B. Göths, S. Möller *et al.* Impact of Kr and Ar seeding on D retention in ferritic-martensitic steels after high-fluence plasma exposure, Nucl. Mater. Energy, 17:307–313, 2018.

[19] Y. Martynova, S. Möller, M. Rasiński, D. Matveev, M. Freisinger *et al.*, Deuterium retention in RAFM steels after high fluence plasma exposure, Nucl. Mater. Energy, 12:648–654, 2017.

[20] V. Kh. Alimov, J. Roth, K. Sugiyama, M. J. Baldwin, R.P. Doerner, Y. Hatano, Deuterium retention in reduced activation ferritic/martensitic steel EUROFER97 exposed to low-energy deuterium plasma, Nucl. Mater. Energy, 35:101430, 2023.

[21] V. Kh Alimov, O.V. Ogorodnikova, Y. Hatano, YuM. Gasparyan, V.S. Efimov *et al.*, Surface modification and deuterium retention in reduced-activation steels exposed to low-energy, high-flux pure and helium-seeded deuterium plasmas, J. Nucl. Mater., 502:1–8, 2018.

[22] E. Malitckii, Y. Yagodzinskyy and H. Hänninen, Hydrogen uptake from plasma and its effect on EUROFER 97 and ODS-EUROFER steels at elevated temperatures, Fusion Eng. Des., 98–99:2025–2029, 2015.

[23] T. Hino, Y. Yamauchi, Y. Kimura, K. Nishimura, Y. Ueda, Fuel hydrogen retention of tungsten and the reduction by inert gas glow discharges, Fusion Eng. Des., 87:876–879, 2012.

[24] S. Ishikawa, K. Katayama, Y. Ohnishi, S. Fukada, M. Nishikawa, Sorption and desorption behavior of hydrogen isotopes from tungsten deposits caused by deuterium gas or deuterium plasma exposure, Fusion Eng. Des., 87:1390–1394, 2012.

[25] E. Malitckii, Y. Yagodzinskyy, M. Ganchenkova, S. Binyukova, H. Hänninen, *et al.*, Comparative study of hydrogen uptake and diffusion in ODS steels, Fusion Eng. Des., 88:2607–2610, 2013.

[26] F. Montupet-Leblond, E.A. Hodille, M. Payet, R. Delaporte-Mathurin, E. Bernard *et al.*, Influence of traps reversibility on hydrogen permeation and retention in Eurofer97, Nucl. Fusion, 62:086011, 2022.

[27] Z. Chen, X. Hu, M. Ye, B. D. Wirth, Deuterium transport and retention properties of representative fusion blanket structural materials, J. Nucl. Mater., 549:152904, 2021.

[28] E. García-Macías, Z. D. Harris and Emilio Martínez-Pañeda, TDS Simulator: A MATLAB App to model temperature-programmed hydrogen desorption, Int. J. Hydrogen Energy, 94:510–524, 2024.

[29] K. Tokunaga, M. J. Baldwin, R. P. Doerner, N. Noda, Y. Kubota *et al.* Blister formation and deuterium retention on tungsten exposed to low energy and high flux deuterium plasma, J. Nucl. Mater. 337–339:887–891, 2005.

[30] M. H. J. 't Hoen, M. Balden, A. Manhard, M. Mayer, S. Elgeti *et al.* Surface morphology and deuterium retention of tungsten after low- and high-flux deuterium plasma exposure, Nucl. Fusion, 54:083014, 2014.

[31] Y. Zayachuk, A. Manhard, M. H. J. 't Hoen, W. Jacob, P. A. Zeijlmans van Emmichoven *et al.*, The effect of ion flux on plasma-induced modification and deuterium retention in tungsten and tungsten–tantalum alloys, J. Nucl. Mater., 464:69–72, 2015,

[32] Z. R. Harutyunyan, Y. M. Gasparyan, V. S. Efimov, S. A. Ryabtsev and A. A. Pisarev, Retention of deuterium in the surface layers of tungsten preliminarily irradiated with helium ions, Bull. Russ. Acad. Sci. Phys. 84:727–731, 2020.